Highly permeable silicon carbide-alumina ultrafiltration membranes for oil-in-water filtration produced with low-pressure chemical vapor deposition

Chen, Mingliang; Shang, Ran; Sberna, Paolo M.; Luiten-Olieman, Mieke W.J. ; Rietveld, Luuk C.; Heijman, Sebastiaan G.J.

DOI
10.1016/j.seppur.2020.117496

Publication date
2020

Document Version
Final published version

Published in
Separation and Purification Technology

Separation and Purification Technology 253 (2020) 117496

Contents lists available at ScienceDirect

Separation and Purification Technology

journal homepage: www.elsevier.com/locate/seppur

Highly permeable silicon carbide-alumina ultrafiltration membranes for oil-in-water filtration produced with low-pressure chemical vapor deposition

Mingliang Chen[a,*], Ran Shang[b], Paolo M. Sberna[c], Mieke W.J. Luiten-Olieman[d], Luuk C. Rietveld[a], Sebastiaan G.J. Heijman[a]

[a] Section of Sanitary Engineering, Department of Water Management, Faculty of Civil Engineering and Geosciences, Delft University of Technology, Stevinweg 1, 2628 CN Delft, the Netherlands
[b] Veolia Water Technologies Techno Center Netherlands B.V., Tanthofdreef 21, 2623 EW Delft, the Netherlands
[c] Else Kooi Laboratory, Delft University of Technology, Feldmannweg 17, 2628 CT Delft, the Netherlands
[d] Inorganic Membranes, MESA+ Institute for Nanotechnology, University of Twente, P.O. Box 217, 7500 AE Enschede, the Netherlands

ARTICLE INFO

Keywords:
Ceramic membranes
Silicon carbide membrane
Low-pressure chemical vapor deposition (LPCVD)
Oil-in-water emulsion

ABSTRACT

Silicon carbide (SiC) ceramic membranes are of particular significance for wastewater treatment due to their mechanical strength, chemical stability, and antifouling ability. Currently, the membranes are prepared by SiC-particle sintering at a high temperature. The production suffers from long production time and high costs. In this paper, we demonstrated a more economical way to produce SiC ultrafiltration membranes based on low-pressure chemical vapor deposition (LPCVD). SiC was deposited in the pores of alumina microfiltration supports using two precursors (SiH_2Cl_2 and C_2H_2/H_2) at a relatively low temperature of 750 °C. Different deposition times varying from 0 to 150 min were used to tune membrane pore size. The pure water permeance of the membranes only decreased from 350 $Lm^{-2}h^{-1}bar^{-1}$ to 157 $Lm^{-2}h^{-1}bar^{-1}$ when the deposition time was increased from 0 to 120 min due to the narrowing of membrane pore size from 71 to 47 nm. Increasing the deposition time from 120 to 150 min mainly resulted in the formation of a thin, dense layer on top of the support instead of in the pores. Oil-in-water emulsion filtration experiments illustrated that both the reversible and irreversible fouling of the SiC-deposited UF membrane was considerably lower as compared to the pristine alumina support. The unique feature that pore sizes decrease linearly as a function of SiC deposition time creates opportunities to produce low-fouling SiC membranes with tuned pore sizes on relatively cheap support.

1. Introduction

In recent years, ceramic membranes, especially microfiltration (MF) and ultrafiltration (UF), have been used for drinking water production and wastewater treatment [1,2]. The mechanical, chemical, and thermal stability of ceramic membranes favours their durable applications in high temperature and corrosive environments where polymeric membranes may not be applicable [3,4]. In addition, ceramic membranes can be chemically cleaned under extreme conditions, after severe fouling, to recover their performance. This can also extend their service lifetime in industrial applications [5].

Among the ceramic membranes, SiC membranes have been extensively studied for high-temperature and high-pressure gas-phase reactive separations, due to their combination of properties such as hardness, chemical resistance, low thermal expansion coefficient and high thermal shock resistance [6,7]. The use of SiC membranes in water purification has been reported as well [5,8–11]. It has been observed that the SiC MF membranes have high water permeance [12–14] and are suitable for long-term applications in slightly oxidative environments such as swimming pool water [9]. Moreover, due to surface characteristics that consist of a combination of super-hydrophilicity and a highly negative charge, SiC membranes exhibit lower reversible and irreversible fouling for surface water and, especially, produced water treatment, when compared with other ceramic and polymeric membranes [5,8].

Pure SiC membranes have been synthesized with various methods such as liquid phase sintering and sintering at low-pressures [15]. However, to form strong covalent Si-C bonds, a high sintering temperature up to 2000 °C in an argon atmosphere and the addition of sintering aids such as Al_2O_3 [16,17] and templates [18] are usually necessary for the production of SiC membranes [19,20]. As a result, the SiC membrane production is quite costly. It is challenging to prepare

* Corresponding author.
E-mail address: M.Chen-1@tudelft.nl (M. Chen).

https://doi.org/10.1016/j.seppur.2020.117496
Received 22 April 2020; Received in revised form 28 July 2020; Accepted 28 July 2020
Available online 02 August 2020

thin SiC layers in the range of ultrafiltration (pores 2–100 nm) or even nanofiltration (pores 1–2 nm) by solid particle sintering, giving rise to limited use of SiC membranes in the water treatment field [21].

Thus, an alternative processing route to prepare SiC UF membranes at reduced temperatures would be required. Up to now, there are mainly two other approaches employed, mostly for SiC gas separation: chemical vapor deposition (CVD) /chemical vapor infiltration (CVI), and pyrolysis of pre-ceramic polymer precursors [22–25]. In CVD/CVI, macroporous α-alumina or SiC membranes are usually used as the supports for the deposition of a thick layer of SiC with one or two precursors at 700–800 °C, followed by a calcination process at 1000 °C in Ar [22,23]. Ciora et al. first reported the preparation of nanoporous hydrogen-selective SiC membranes on γ-Al_2O_3 tubular supports by using CVD with the two precursors tri-isopropylsilane (TPS) and 1,3-disilabutane (DSB) [24]. Despite both precursors can produce nanoporous membranes, a high-temperature post-treatment was necessary to improve the H_2 permeance and H_2/H_2O selectivity. In the second approach, a dip-coating technique through the pyrolysis of allyl-hydridopolycarbosilane (AHPCS) has also been developed by Ciora et al. [24]. Membranes prepared by polycarbosilane (PCS) pyrolysis at 600 °C gave satisfactory H_2 permeance despite a relatively low H_2/N_2 selectivity. However, due to the film shrinkage during the conversion of the polymer precursors to SiC, this method had to be repeated several times to obtain a defect-free film [21,26]. Although it is thus feasible with both reported methods to prepare SiC nanoporous membranes at lower temperatures, the prepared membranes usually have a thick SiC layer, which negatively affects the water permeance and, therefore, they are predominately limited for the purpose of gas-separation applications. More recently, Konig et al. developed UF SiC membranes on macroporous SiC supports by coating a suspension of α-SiC powder and AHPCS in n-hexane or n-hexane/n-tetradecane. The prepared membranes showed a defect-free mesoporous surface, but still, quite low water permeance (0.05–0.06 $Lm^{-2}h^{-1}bar^{-1}$) was observed [21].

It thus remains a challenge to produce SiC UF membranes at low temperatures with high water permeance, especially for oil-in-water emulsion separation, which is usually affected by severe fouling problems when using other ceramic and polymeric membranes [19]. Recent studies have shown that the fabrication of ultrathin SiC membranes by means of low-pressure chemical vapor deposition (LPCVD) is a promising platform for cell culturing [27]. To the best of our knowledge, the fabrication of SiC UF membranes via LPCVD has not been realized yet. Therefore, in this work, LPCVD was used to deposit a thin layer of SiC in the pores of commercial ceramic alumina membranes with the objective to use them for oil-in-water emulsion filtration with reduced membrane fouling.

2. Materials and methods

2.1. Materials

Commercial tubular ceramic membranes (CoorsTek, the Netherlands) with an inner diameter of 7 mm and an outer diameter of 10 mm were used as support for LPCVD deposition. These membranes are composed of a selective layer of α-alumina with a pore size of 100 nm (specification of the manufacturer) on macroporous α-alumina support. The membranes have an average pure water flux of 382 $Lm^{-2}h^{-1}bar^{-1}$, as given by the manufacturer. However, great variations in actual permeance were observed during the tests (20 tubes). Therefore, only the membranes with similar permeance, being around 350 $Lm^{-2}h^{-1}bar^{-1}$, were chosen for the LPCVD deposition.

2.2. Low-pressure chemical vapor deposition

The membrane tubes were cut into 15 cm long segments to fit the LPCVD chamber. The SiC layer was deposited onto the support, both on the inner and outer surface, in a hot-wall LPCVD furnace (Tempress Systems BV, the Netherlands), as shown in Fig. 1. Dichlorosilane (SiH_2Cl_2) and acetylene (C_2H_2), diluted at 5% in hydrogen (H_2), were used as precursors, respectively. The purging gas, employed in the system, was ultrapure nitrogen (N_2), obtained from a liquid nitrogen source. In the reactor, the support membranes were placed in the center of the chamber with their long-axis parallel to the precursors' flow direction.

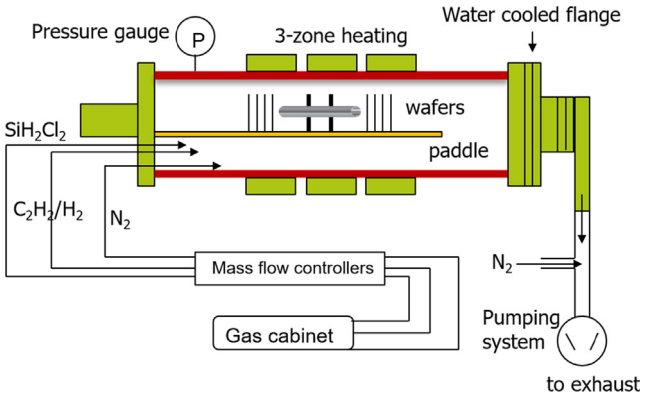

Fig. 1. Schematic of the LPCVD system used for the membrane deposition of SiC layers.

The deposition parameters, temperature, and pressure were selected based on the study of Morana et al. [28] on wafers, to obtain a thin and continuous amorphous SiC layer on the membrane surface. Therefore, the depositions were performed at a temperature of 750 °C and pressure of 60 Pa. In addition, a gas flow ratio (SiH_2Cl_2 to C_2H_2) of 3 with a total gas flow of 500 sccm was chosen, while the deposition time was varied between 0 and 150 min to tune layer thickness and membrane pore size. In order to simplify the sample names, all samples are labeled as Dx, where x represents the deposition time (x = 0, 60, 90, 120, and 150 min).

During the deposition, silicon wafers with a diameter of 100 mm and a thickness of 525 (± 25) μm were placed next to the membranes to monitor the deposited layer thickness. The layer thickness was later determined by an ellipsometer (M-2000UI, J.A. Woollam Co. Inc., USA), based on the change of the light polarization principle [29]. Additionally, the growth rate of the SiC layer, obtained through linear regression between layer thickness and the deposition time, was used to estimate the rate of pore size change of the membrane.

2.3. Membrane characterization

The morphology of the pristine alumina and LPCVD modified SiC-alumina membranes were observed by scanning electron microscopy (SEM, FEI Nova NanoSEM 450, USA). The Si/Al intensity ratios of the samples were determined using energy dispersive X-ray (EDX) analyzer (Ametek $EDAX^{TSL}$) at 10 kV accelerating voltage, which is coupled in an SEM-EDX system. Prior to observation, membrane samples were sputtered with a thin layer of gold to increase sample conductivity, which is necessary to obtain a clear image. The average pore size and pore size distribution of the membranes were measured by capillary flow porometry (Porolux 500, IBFT GmbH, Germany). FC43 (Benelux Scientific B.V., the Netherlands) was used as the wetting agent for porometry measurements, and the flow and feed pressure were recorded in time. The pore size and pore size distribution were then calculated using the Young-Laplace equation [30]:

$$D = \frac{4\gamma \cdot cos\theta \cdot SF}{P} \quad (1)$$

where D is the pore diameter of the membrane (m), γ is the surface tension of the wetting liquid (N/m), θ is the contact angle of the liquid on the membrane surface (0°), P is the used pressure (bar), and SF is the

shape factor ($SF = 1$).

The water flux of the membrane before and after deposition was examined, filtering demineralized water at a constant transmembrane pressure (TMP) of 1.5 bar. Membrane fluxes and the water temperature were monitored every 30 s. In order to compare the membrane water permeance, all membrane permeance were corrected to the equivalent at 20 °C using the following equation (2) [29]:

$$L_{p,20\,^{\circ}\mathrm{C}} = \frac{J \cdot e^{-0.0239 \cdot (T-20)}}{\Delta P} \quad (2)$$

where $L_{p,20\ ^{\circ}C}$ is the permeance at 20 °C ($Lm^{-2}h^{-1}bar^{-1}$), J is the measured membrane flux ($Lm^{-2}h^{-1}$), ΔP is the measured TMP (bar), T is the temperature of water (°C).

2.4. Oil-in-water emulsion preparation

To ensure that all oil-in-water emulsions had the same characteristics during all experiments, a stock emulsion was prepared, which was then diluted to the desired oil concentration. The stock emulsion was prepared by mixing 3 mL mineral oil (Sigma-Aldrich) and 0.6 g sodium dodecyl sulphate (SDS) (Sigma-Aldrich) with 2 L of demineralized water. This stock emulsion was continuously stirred with a magnetic stirrer (L23, LABINCO, the Netherlands) at a speed of 1500 rpm for 36 h and then ultrasonicated (521, Bransonic, US) for 2 h until it appeared milky white. The emulsion did not segregate for 3 days, indicating good stability and homogeneity. Afterward, the emulsion was diluted to 6 L with a concentration of 400 ppm for the filtration experiments. The used oil concentration was in the normal range typically observed in oily wastewater [31]. The emulsion has a pH of around 6 measured by a pH sensor (inoLab™ Multi 9420 - WTW). The oil droplet size distribution was analyzed with a particle size analyzer (Bluewave, Microtrac, USA), and the average oil droplet size of the emulsion was 2 μm (Fig. S1, supporting information).

2.5. Constant flux crossflow fouling experiments with backwash

The membrane filtration set-up with backwash was designed for constant flux experiments (Fig. 2). The system contained a feed pump (DDA12-10, Grundfos, Denmark) to dose the emulsion into the circulation loop and to control the permeate flux, and a circulation pump (VerderGear, Verder B.V., the Netherlands) to provide a fixed crossflow velocity of 0.44 m/s, monitored by a flow meter (YF-S402, Zhongjiang energy-efficient electronics Co., Itd., China). A backwashing vessel, filled with demineralized water, was connected to a compressed air system, and a fixed pressure of 3 bar was set for backwashing. Two high-precision pressure transducers (GS4200-USB, ESI, UK) were installed on the two sides of the membrane module to monitor the pressure variations. Since the pressure of the permeate stream was equal to atmospherical, the pressure exhibited by the pressure transducers was TMP. A digital balance (KERN EWJ 600, Germany) was used to measure the permeate flux in case there was a difference with the feed pump flow. During the experiments, the pressure, temperature and flow were continuously logged at a time interval of 30 s.

The pristine (D0) and modified (D120) membranes were tested separately with the above mentioned constant flux filtration set-up to compare the membrane fouling resistance before and after deposition. A new membrane was used for each test. The oil-in-water emulsion was used as a model foulant in this study. All filtration experiments were done at room temperature (22 °C) and carried out in duplicate. Prior to each filtration experiment, the membranes were immersed in demineralized water overnight to wet all the pores. The set-up was thoroughly flushed with demineralized water to remove residual chemicals and air in the system. Afterward, the initial permeance of each membrane was determined with demineralized water at a constant flux of 100 $Lm^{-2}h^{-1}$ for 10 min. Each fouling experiment consisted of 7 cycles, and each cycle was composed of three phases in the following order: 1) Filtration of oil-in-water emulsion at a constant flux of 100 $Lm^{-2}h^{-1}$ for 18 min, 2) Backwashing the membrane module with demineralized water at a fixed pressure of 3 bar for 30 s to remove the hydraulically reversible fouling, 3) Forward flush with feed for 15 s at a crossflow velocity of 0.44 m/s. The purpose of the forward flush is to purge the membrane module to remove the backwash remaining liquids and replace the solution in the loop with the fresh feed. The explanation to choose a constant flux of 100 $Lm^{-2}h^{-1}$, filtration time of 18 min and a crossflow velocity of 0.44 m/s is given in the supporting information (Fig. S2 and S3). The filtration-backwash-forward flush phase is shown

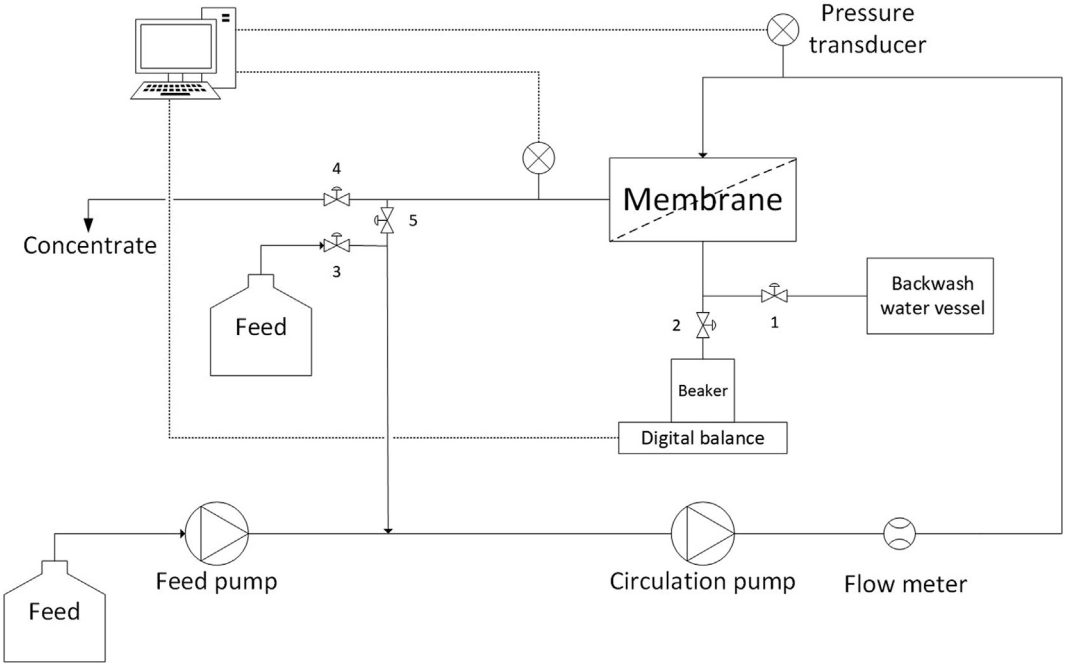

Fig. 2. Schematic view of the filtration set-up. During the experiment, the feed pump was always at a flow of 0.3 L/h, the effective filtration area of the membrane is 0.003 m^2 and the membrane had a constant flux of 100$Lm^{-2}h^{-1}$.

in Table S1.

During the constant flux filtration experiment, the TMP increases in time due to membrane fouling by oil droplets. In order to better compare the membrane performance before and after deposition, the TMP and permeance (P) of the membranes during filtration were normalized to the initial TMP_0 and P_0, which were measured by filtering demineralized water.

The membrane resistance was calculated based on the resistance-in-series model [32,33], as shown in equation (3):

$$R_t = \frac{TMP}{\mu J} = R_m + R_r + R_{ir} \tag{3}$$

where J is the membrane flux (m/s), TMP is the applied *trans*-membrane pressure (Pa), μ is the viscosity of the permeate (Pa·s), R_t (m^{-1}) represents the total resistance, which is consist of intrinsic membrane resistance (R_m), hydraulically reversible resistance (R_r), and irreversible unphysical removable resistance (R_{ir}). R_m was determined through the filtration of demineralized water and R_t was measured according to the final filtration pressure of wastewater. The fouled membrane was backwashed with demineralized water under a pressure of 3 bar and then R_r was measured. The R_{ir} was calculated from R_t - R_r - R_m.

3. Results and discussion

3.1. Thickness and growth kinetics of SiC layers on a silicon wafer

The growth rate of the SiC layer in the pores of the porous ceramic membrane could not be measured directly. To have an indication of the growth rate, silicon wafers were used as substrates to measure the SiC layer thickness with ellipsometry. The results (Fig. 3) show a linear relationship between the deposition time and SiC layer thickness. The growth rate is determined from the slope of the linear regression and is 0.3 nm/min.

Wang and Tsai also studied the SiC deposition with LPCVD and observed a growth rate of 0.87 nm/min, which is higher than the one we found, probably due to the higher pressure in the reaction system they used [34]. The growth rate we found was also much lower than that of plasma-enhanced chemical vapor deposition (PECVD), though deposited at much lower temperatures (200–400 °C) [35,36]. However, a lower growth rate could lead to better control of the film thickness on the target substrates, which is especially important for membrane modification, where uniform deposition into pores is of importance [22].

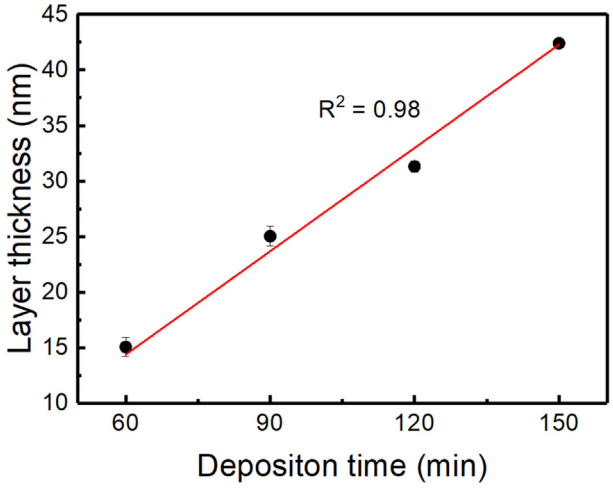

Fig. 3. Correlation between the thickness of the deposited SiC layer and deposition time onto a silicon wafer.

3.2. Morphological evolution of membranes under various deposition times

The cross-section structure of the pristine membrane was analyzed using a scanning electron microscope. The separation layer of the membranes had a thickness of around 25 μm as clearly observed in Fig. 4, but variations from 21 to 25 μm were found for the various samples (Fig. S4).

In Fig. 5, SiC-deposited tubes with various deposition times and one pristine alumina tube (D0) are depicted, showing a change of color from white to brown and black after increasing SiC deposition time. Black is a typical color for a SiC membrane, indicating that the alumina membrane samples were deposited with a homogeneous layer of SiC after around 90 min. Also the inside of the tubes, deposition time 90 min or longer, were examined after breaking, and display uniform colored black surface as well. The inside of the deposited tube's wall, though, was white, indicating that the deposition penetrated only a small part of the alumina tube's wall (see lower right in Fig. 5).

The surface morphologies of the pristine and deposited alumina membranes were further investigated by SEM observations. In Fig. 6, surface SEM images of the pristine ceramic membrane and SiC-deposited ceramic membranes (different deposition times) are shown. The images demonstrate that no continuous SiC layer is deposited on top of the support membrane's surface but the SiC is mainly deposited in the pores. It also shows that prolongation of the deposition time, from 60 to 150 min, results in a considerable decrease in pore size.

In addition, longer deposition times allow the precursors, dichlorosilane and acetylene, to diffuse more in-depth into the support. To study the effect of the penetration of the precursors on the membrane's morphology, cross-sectional SEM pictures of the membranes were made (Fig. 7). From Fig. 7C it can be observed that after 90 min a SiC layer started to be formed on top of the top layer, while after 150 min, it appeared to cover the entire top layer.

SEM-EDX line scans were made to provide elemental identification of the SiC deposition in the pores. The results are depicted in Fig. 7F, showing the Si/Al intensity ratios of the pristine alumina membrane and the different SiC-deposited membranes as a function of the distance from the membrane surface. In the first 90 min the gas diffuses around 10 μm into the top layer of the support and after 120 min SiC was deposited in the pores of the entire support's top layer. It looks like there is less infiltration after 150 min as compared to 120 min. This could be caused by a variation in the thickness of the top layer. Fig. S4 shows that the supports' top layer varied between 21 and 25 μm so it means that after 120 min SiC is already deposited in the pores of the entire top layer. In the initial period of LPCVD deposition (0–120 min), the pores among particles were large enough to allow rapid and unlimited diffusion of precursors into the pores, and sufficient adsorption and reaction happened on the particle surface. With further increase of the deposition time, the diffusion of the precursors into the pores would be restricted due to the narrowing pore mouth. Thus, the deposition rate of SiC layer inside the pores reduced after 120 min. As a result, deposition mainly happened on the top surface and resulted in the addition of a new, dense thin film. Similar profiles have been observed by Jolien et al. and Roy et al. [37,38]. Overall, these above-mentioned discussions revealed that the LPCVD is an effective conformal deposition technique over complex three-dimensional structures like the tubular membranes used in our work.

3.3. Effect of LPCVD deposition on pure water flux and membrane pore size

Pure water permeance tests were conducted on both the pristine membranes and the LPCVD modified membranes after different deposition times. The results of the pure water permeance test are displayed in Fig. 8a. The permeance of the membranes decreased linearly from 350 $Lm^{-2}h^{-1}bar^{-1}$ to 157 $Lm^{-2}h^{-1}bar^{-1}$ when the deposition time was increased from 0 min to 120 min. After 120 min the decline in permeance was lower.

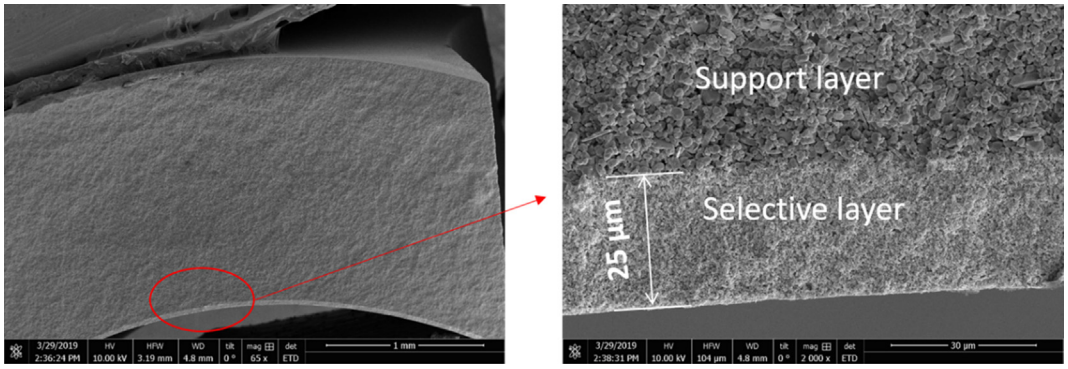

Fig. 4. SEM images of the cross-section of the pristine alumina membrane.

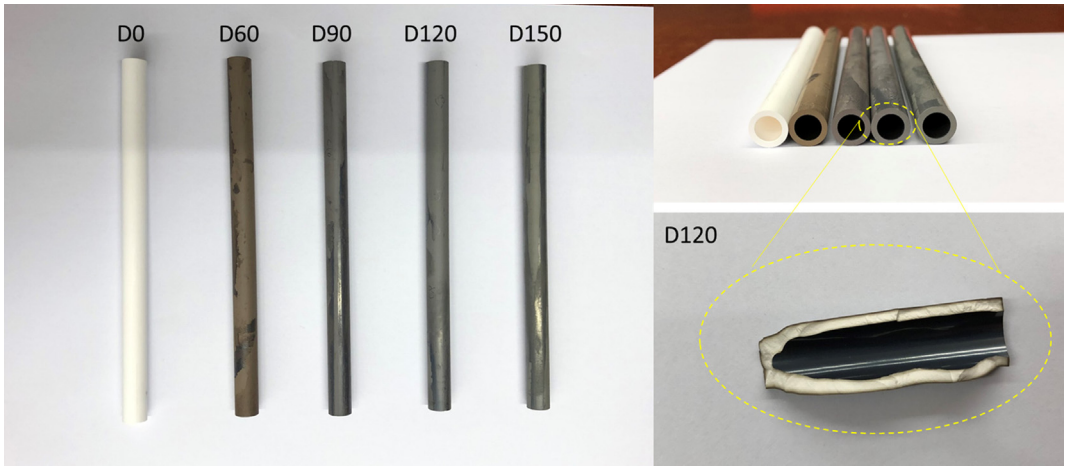

Fig. 5. Photos of the pristine membrane and LPCVD modified membranes.

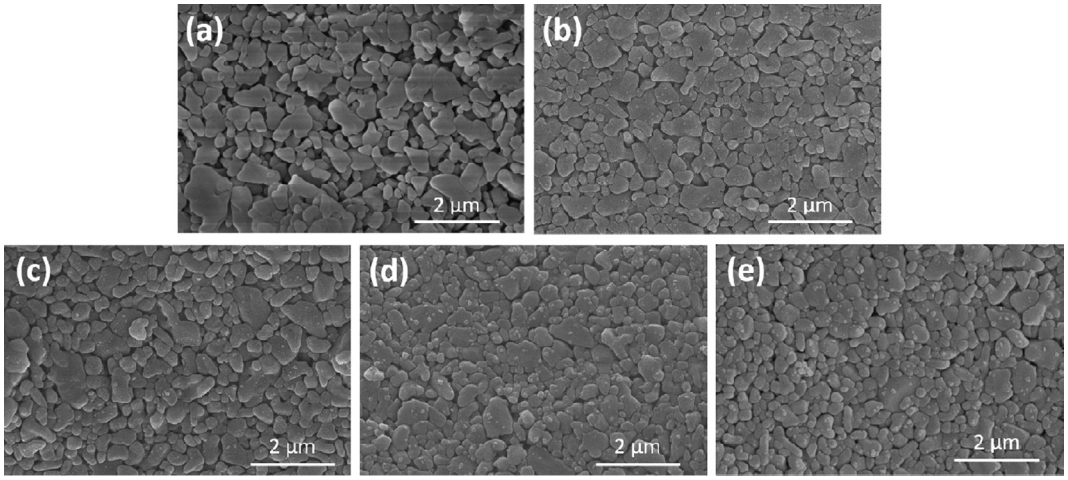

Fig. 6. Surface SEM images of (a) the pristine ceramic membrane (D0), and SiC-deposited ceramic membranes with increasing deposition times: (b) D60, (c) D90, (d) D120, (e) D150.

Pore size measurements of the pristine alumina membrane and the LPCVD modified membranes were performed and the results are shown in Fig. 8b. The alumina membrane, black line in Fig. 8b, had a broad pore size distribution, and contained pores between 40 and 80 nm with an average of 71 nm. Compared to the pristine membrane, the deposited membranes had a narrower pore size distribution and smaller average pore sizes. A substantial decline in pore size was observed with increased deposition time, from 71 nm to 43 nm after 150 min of SiC deposition. Fig. 8c demonstrates that the pore diameter decline was linear except the pore size measured after 60 min of deposition, where a slight deviation from the line can be observed. The phenomenon of the linear permeance and pore size decline has also been described in previous studies [22,39], where CVD was used to modify the membranes. As the water permeance decreased with the same slope, we assume that something went wrong during the pore size measurement of the tube with a deposition time of 60 min.

3.4. Filtration of an oil-in-water emulsion

The SiC-deposited membrane with 120 min deposition time (D120)

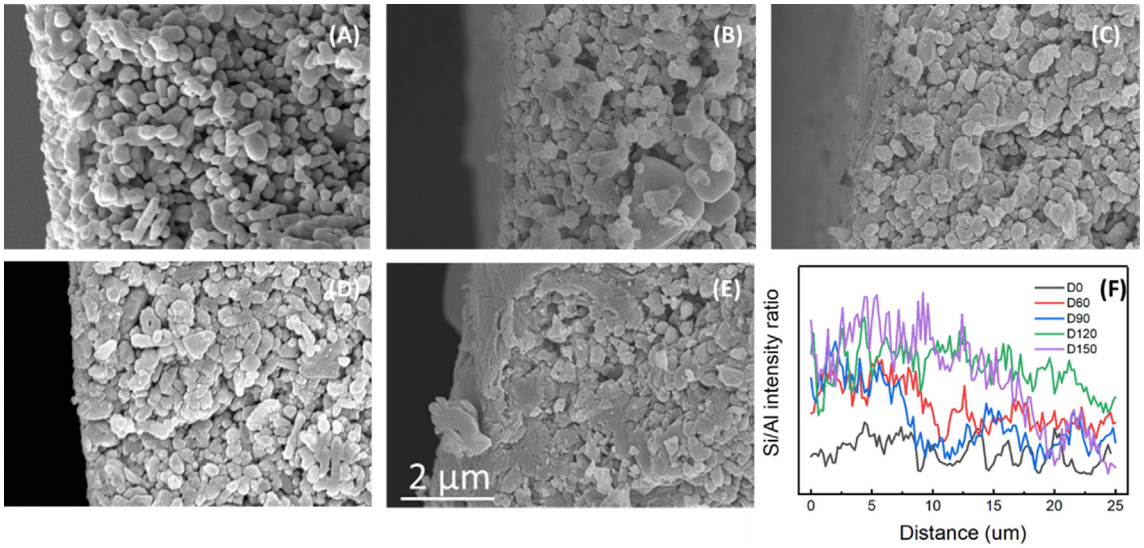

Fig. 7. The cross-sectional SEM images of the pristine and LPCVD modified membranes: D0 (A), D60 (B), D90 (C), D120 (D), D150 (E) and corresponding line-scan EDX spectra (F). All images have the same magnification and the scale bar is shown in (E).

and the pristine alumina membrane (D0) were compared with respect to the filtration of an oil-in-water emulsion. The initial permeance of both membranes for emulsion filtration were close to their pure water permeance, indicating the membranes were not fouled at the initial stage (Fig. S5). To better compare the membrane performance, we normalized the TMP and permeance. In Fig. 9a the normalized TMP is visualized as a function of the filtration time, showing a fast increase in the relative TMP of both D0 and D120 during one filtration cycle, indicating that considerable fouling occurred in both membranes. However, the pristine alumina membrane maintained a high TMP increase rate during all filtration cycles. In contrast, a much slower TMP increase was observed for the SiC-deposited membrane with 120 min deposition time. The final relative TMP of D0 was more than 1.5 times higher than that of D120, suggesting fouling was much less after modification.

At the end of each cycle, the membranes were hydraulically

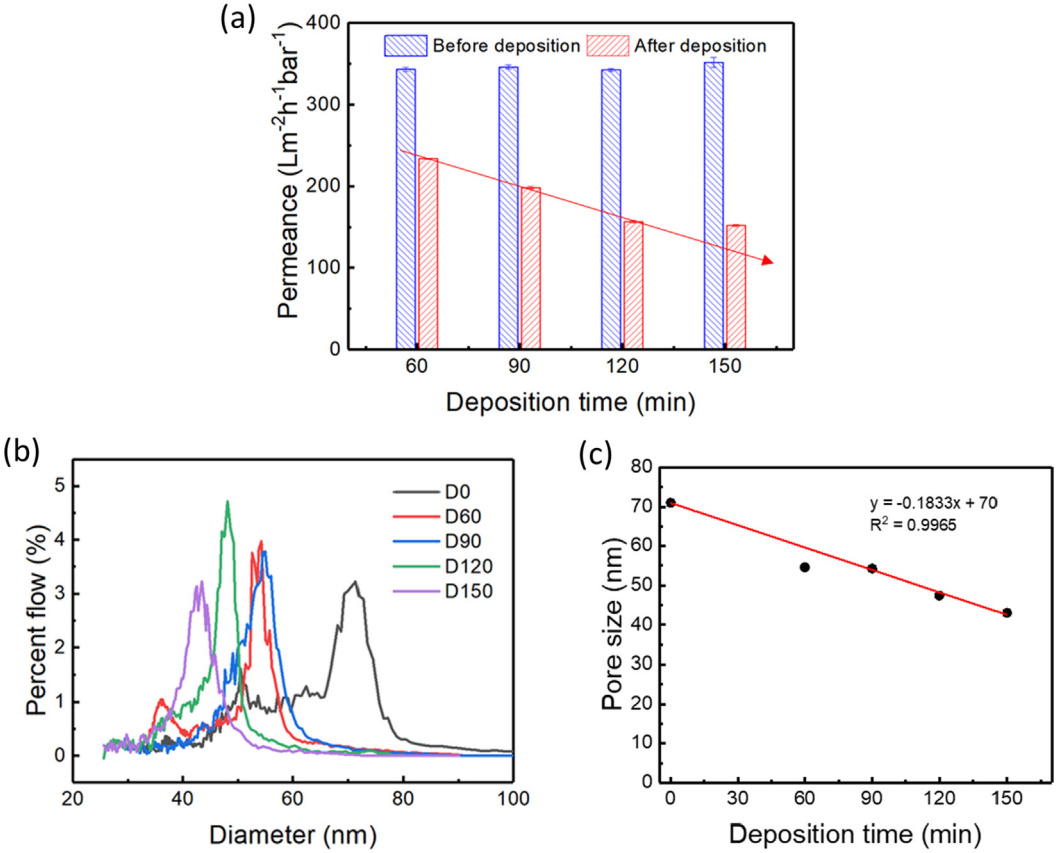

Fig. 8. (a) Pure water permeance and (b) pore size distribution of pristine membrane and LPCVD modified membranes; (c) linear fit of pore size variations with deposition time (D60 is not included).

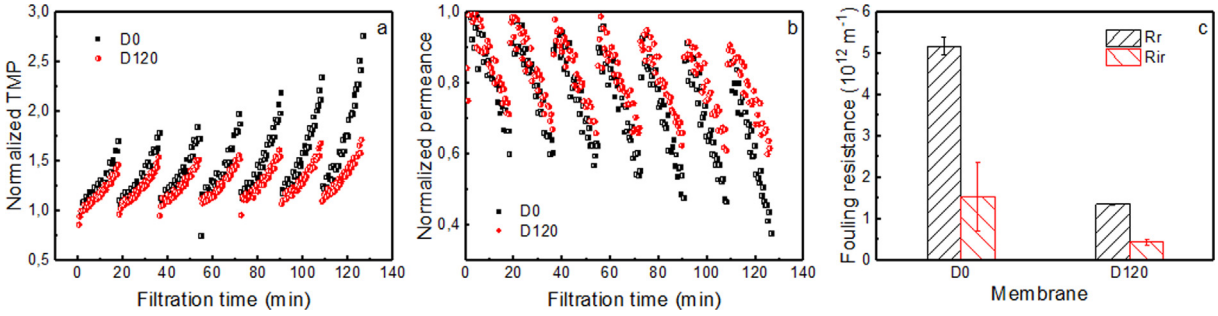

Fig. 9. (a) Normalized TMP, (b) normalized permeance, and (c) fouling resistance of D0 and D120 for oil-in-water emulsion filtration.

backwashed with demineralized water before starting the next filtration cycle. It was found that the permeance of both membranes (Fig. 9b) was only slightly reduced after the first backwashing, indicating the reversible fouling was mainly responsible for the permeance loss. The gradual development of irreversible fouling was observed for both membranes during subsequent filtration cycles. To further reveal the influence of the SiC-deposited layer on fouling mitigation, the resistance distribution during the filtration process was analyzed. Fig. 9c shows the reversible and irreversible fouling resistance for both membranes during the entire filtration process. Both the reversible and irreversible fouling resistance of D120 was smaller than that of D0, indicating that the SiC-deposited layer mitigated the membrane fouling during oil-in-water emulsion filtration. Based on the above discussions, it can be concluded that the SiC-deposited membrane was less prone to fouling as compared to the pristine membrane for oil-in-water emulsion filtration.

The pore sizes of D0 and D120 are much smaller than the average size of the oil droplets. Therefore, it is assumed that the surface properties of the SiC-deposited layer are the most important in avoiding fouling. Previous studies also showed that SiC membranes have a low fouling tendency as compared to other ceramic and polymeric membranes, which is closely related to super hydrophilicity [8] and the low *iso*-electric point (pH 2.8) of SiC [9]. The pristine alumina membrane has a relatively high *iso*-electric point which is about 9 [40]. The emulsion used in this study had a pH of 6, which means that the modified membrane surface was negatively charged while the pristine membrane had a positive surface charge during the filtration process. The emulsion also had a highly negative charge due to the negative charge of the surfactant (SDS) surrounding the oil droplet [41]. Therefore, electrostatic-interaction would be different for the two membranes, and the SiC layer of the modified membrane would protect the membrane from adsorbing or depositing oil droplets not only due to the hydrophilic characteristics of the surface, but also because of electrostatic repulsion forces between the membrane surface and oil droplets. In contrast, electrostatic adhesion could happen on alumina membrane surface due to the opposite charge between membrane surface and oil droplets which would accelerate membrane fouling.

4. Conclusion

In this work, tubular SiC UF membranes with pore sizes between 43 and 55 nm were manufactured on an alumina supporting tube via low-pressure chemical vapor deposition, a straightforward and more economical method to produce SiC UF membranes. Pure water permeance of the modified membranes decreased linearly until a deposition time of 120 min from 350 $Lm^{-2}h^{-1}bar^{-1}$ to 157 $Lm^{-2}h^{-1}bar^{-1}$. Pore size measurements also depicted a linear decline in pore size with increasing deposition time (confirmed by SEM images). Deposition times longer than 120 min mainly resulted in the addition of a thin, dense selective layer on top of the support. The developed SiC-deposited UF membranes show a low fouling characteristic and a small permeance loss during oil-in-water emulsion filtration, probably due to a combination of hydrophilic and charge interactions. These findings create opportunities to produce low fouling SiC membranes with tuned pore sizes on relatively cheap support.

CRediT authorship contribution statement

Mingliang Chen: Conceptualization, Methodology, Investigation, Data curation, Writing - original draft. **Ran Shang:** Resources, Methodology. **Paolo M. Sberna:** Methodology, Formal analysis. **Mieke W.J. Luiten-Olieman:** Data curation, Writing - review & editing, Supervision. **Luuk C. Rietveld:** Writing - review & editing. **Sebastiaan G.J. Heijman:** Writing - review & editing, Conceptualization, Resources, Supervision.

Declaration of Competing Interest

The authors declare that they have no known competing financial interests or personal relationships that could have appeared to influence the work reported in this paper.

Acknowledgements

Mingliang Chen acknowledges the China Scholarship Council for his PhD scholarship under the State Scholarship Fund (No. 201704910894). We appreciate Prof. Louis Winnubst (University of Twente) for the valuable suggestions on the manuscript and thank Dr. B. Morana (Delft University of Technology) for the help on SiC deposition.

Appendix A. Supplementary material

Supplementary data to this article can be found online at https://doi.org/10.1016/j.seppur.2020.117496.

References

[1] M. Chen, L. Zhu, J. Chen, F. Yang, C.Y. Tang, M.D. Guiver, Y. Dong, Spinel-based ceramic membranes coupling solid sludge recycling with oily wastewater treatment, Water Res. 169 (2020) 115180.
[2] A. Kayvani Fard, G. McKay, A. Buekenhoudt, H. Al Sulaiti, F. Motmans, M. Khraisheh, M. Atieh, Inorganic membranes: preparation and application for water treatment and desalination, Materials (Basel) 11 (2018).
[3] M. Chen, L. Zhu, Y. Dong, L. Li, J. Liu, Waste-to-resource strategy to fabricate highly porous whisker-structured mullite ceramic membrane for simulated oil-in-water emulsion wastewater treatment, ACS Sustain. Chem. Eng. 4 (2016) 2098–2106.
[4] H. Chen, X. Jia, M. Wei, Y. Wang, Ceramic tubular nanofiltration membranes with tunable performances by atomic layer deposition and calcination, J. Membr. Sci. 528 (2017) 95–102.
[5] C. He, R.D. Vidic, Application of microfiltration for the treatment of Marcellus Shale flowback water: Influence of floc breakage on membrane fouling, J. Membr. Sci. 510 (2016) 348–354.
[6] S.C. Kim, H.J. Yeom, Y.W. Kim, I.H. Song, J.H. Ha, Processing of alumina-coated glass-bonded silicon carbide membranes for oily wastewater treatment, Int. J. Appl. Ceram. Tec. 14 (2017) 692–702.
[7] S. Dabir, W. Deng, M. Sahimi, T. Tsotsis, Fabrication of silicon carbide membranes on highly permeable supports, J. Membr. Sci. 537 (2017) 239–247.

[8] B. Hofs, J. Ogier, D. Vries, E.F. Beerendonk, E.R. Cornelissen, Comparison of ceramic and polymeric membrane permeability and fouling using surface water, Sep. Purif. Technol. 79 (2011) 365–374.
[9] B. Skibinski, P. Müller, W. Uhl, Rejection of submicron sized particles from swimming pool water by a monolithic SiC microfiltration membrane: Relevance of steric and electrostatic interactions, J. Membr. Sci. 499 (2016) 92–104.
[10] T. Zsirai, A.K. Al-Jaml, H. Qiblawey, M. Al-Marri, A. Ahmed, S. Bach, S. Watson, S. Judd, Ceramic membrane filtration of produced water: Impact of membrane module, Sep. Purif. Technol. 165 (2016) 214–221.
[11] M.C. Fraga, S. Sanches, J.G. Crespo, V.J. Pereira, Assessment of a new silicon carbide tubular honeycomb membrane for treatment of olive mill wastewaters, Membranes (Basel) 7 (2017).
[12] M. Facciotti, V. Boffa, G. Magnacca, L.B. Jørgensen, P.K. Kristensen, A. Farsi, K. König, M.L. Christensen, Y. Yue, Deposition of thin ultrafiltration membranes on commercial SiC microfiltration tubes, Ceram. Int. 40 (2014) 3277–3285.
[13] P. de Wit, E.J. Kappert, T. Lohaus, M. Wessling, A. Nijmeijer, N.E. Benes, Highly permeable and mechanically robust silicon carbide hollow fiber membranes, J. Membr. Sci. 475 (2015) 480–487.
[14] J.-H. Eom, Y.-W. Kim, I.-H. Song, Effects of the initial α-SiC content on the microstructure, mechanical properties, and permeability of macroporous silicon carbide ceramics, J. Eur. Ceram. Soc. 32 (2012) 1283–1290.
[15] W. Deng, X. Yu, M. Sahimi, T.T. Tsotsis, Highly permeable porous silicon carbide support tubes for the preparation of nanoporous inorganic membranes, J. Membr. Sci. 451 (2014) 192–204.
[16] Y. Zhou, M. Fukushima, H. Miyazaki, Y.-I. Yoshizawa, K. Hirao, Y. Iwamoto, K. Sato, Preparation and characterization of tubular porous silicon carbide membrane supports, J. Membr. Sci. 369 (2011) 112–118.
[17] D. Das, S. Baitalik, B. Haldar, R. Saha, N. Kayal, Preparation and characterization of macroporous SiC ceramic membrane for treatment of waste water, J. Porous Mater. 25 (2018) 1183–1193.
[18] J.-H. Eom, Y.-W. Kim, Effect of template size on microstructure and strength of porous silicon carbide ceramics, J. Ceram. Soc. Jpn. 116 (2008) 1159–1163.
[19] M.C. Fraga, S. Sanches, V.J. Pereira, J.G. Crespo, L. Yuan, J. Marcher, M.V.M. de Yuso, E. Rodríguez-Castellón, J. Benavente, Morphological, chemical surface and filtration characterization of a new silicon carbide membrane, J. Eur. Ceram. Soc. 37 (2017) 899–905.
[20] W. Wei, W. Zhang, Q. Jiang, P. Xu, Z. Zhong, F. Zhang, W. Xing, Preparation of non-oxide SiC membrane for gas purification by spray coating, J. Membr. Sci. 540 (2017) 381–390.
[21] K. König, V. Boffa, B. Buchbjerg, A. Farsi, M.L. Christensen, G. Magnacca, Y. Yue, One-step deposition of ultrafiltration SiC membranes on macroporous SiC supports, J. Membr. Sci. 472 (2014) 232–240.
[22] L.L. Lee, D.S. Tsai, Silicon carbide membranes modified by chemical vapor deposition using species of low sticking coefficients in a silane/acetylene reaction system, J. Am. Ceram. Soc. 81 (1998) 159–165.
[23] B.-K. Sea, K. Ando, K. Kusakabe, S. Morooka, Separation of hydrogen from steam using a SiC-based membrane formed by chemical vapor deposition of triisopropylsilane, J. Membr. Sci. 146 (1998) 73–82.
[24] R.J. Ciora, B. Fayyaz, P.K.T. Liu, V. Suwanmethanond, R. Mallada, M. Sahimi, T.T. Tsotsis, Preparation and reactive applications of nanoporous silicon carbide membranes, Chem. Eng. Sci. 59 (2004) 4957–4965.
[25] B. Elyassi, M. Sahimi, T.T. Tsotsis, Silicon carbide membranes for gas separation applications, J. Membr. Sci. 288 (2007) 290–297.
[26] P. Colombo, G. Mera, R. Riedel, G.D. Soraru, Polymer-derived ceramics: 40 years of research and innovation in advanced ceramics, J. Am. Ceram. Soc. 93 (2010) 1805–1837.
[27] T.-K. Nguyen, H.-P. Phan, H. Kamble, R. Vadivelu, T. Dinh, A. Iacopi, G. Walker, L. Hold, N.-T. Nguyen, D.V. Dao, Superior robust ultrathin single-crystalline silicon carbide membrane as a versatile platform for biological applications, ACS Appl. Mater. Interfaces 9 (2017) 41641–41647.
[28] B. Morana, G. Pandraud, J.F. Creemer, P.M. Sarro, Characterization of LPCVD amorphous silicon carbide (a-SiC) as material for electron transparent windows, Mater. Chem. Phys. 139 (2013) 654–662.
[29] R. Shang, A. Goulas, C.Y. Tang, X. de Frias Serra, L.C. Rietveld, S.G.J. Heijman, Atmospheric pressure atomic layer deposition for tight ceramic nanofiltration membranes: Synthesis and application in water purification, J. Membr. Sci. 528 (2017) 163–170.
[30] R. Shang, F. Vuong, J. Hu, S. Li, A.J.B. Kemperman, K. Nijmeijer, E.R. Cornelissen, S.G.J. Heijman, L.C. Rietveld, Hydraulically irreversible fouling on ceramic MF/UF membranes: Comparison of fouling indices, foulant composition and irreversible pore narrowing, Sep. Purif. Technol. 147 (2015) 303–310.
[31] N.A. Ahmad, P.S. Goh, Z. Abdul Karim, A.F. Ismail, Thin film composite membrane for oily waste water treatment: recent advances and challenges, Membranes 8 (2018) 86.
[32] B.-C. Huang, Y.-F. Guan, W. Chen, H.-Q. Yu, Membrane fouling characteristics and mitigation in a coagulation-assisted microfiltration process for municipal wastewater pretreatment, Water Res. 123 (2017) 216–223.
[33] J. Xing, H. Liang, C.J. Chuah, Y. Bao, X. Luo, T. Wang, J. Wang, G. Li, S.A. Snyder, Insight into Fe (II)/UV/chlorine pretreatment for reducing ultrafiltration (UF) membrane fouling: Effects of different natural organic fractions and comparison with coagulation, Water Res. 167 (2019) 115112.
[34] C.-F. Wang, D.-S. Tsai, Low pressure chemical vapor deposition of silicon carbide from dichlorosilane and acetylene, Mater. Chem. Phys. 63 (2000) 196–201.
[35] C. Iliescu, B. Chen, J. Wei, A.J. Pang, Characterisation of silicon carbide films deposited by plasma-enhanced chemical vapour deposition, Thin Solid Films 516 (2008) 5189–5193.
[36] C. Iliescu, B. Chen, D.P. Poenar, Y.Y. Lee, PECVD amorphous silicon carbide membranes for cell culturing, Sensor. Actuat. B: Chem. 129 (2008) 404–411.
[37] R.G. Gordon, D. Hausmann, E. Kim, J. Shepard, A kinetic model for step coverage by atomic layer deposition in narrow holes or trenches, Chem. Vap. Deposition 9 (2003) 73–78.
[38] J. Dendooven, D. Deduytsche, J. Musschoot, R. Vanmeirhaeghe, C. Detavernier, Conformality of Al2O3 and AlN deposited by plasma-enhanced atomic layer deposition, J. Electrochem. Soc. 157 (2010) G111–G116.
[39] Y. Lin, A. Burggraaf, Experimental studies on pore size change of porous ceramic membranes after modification, J. Membr. Sci. 79 (1993) 65–82.
[40] C. Atallah, A.Y. Tremblay, S. Mortazavi, Silane surface modified ceramic membranes for the treatment and recycling of SAGD produced water, J. Petrol. Sci. Eng. 157 (2017) 349–358.
[41] Y.-M. Lin, G.C. Rutledge, Separation of oil-in-water emulsions stabilized by different types of surfactants using electrospun fiber membranes, J. Membr. Sci. 563 (2018) 247–258.